# KAWASAKI WAKE SURVEY SYSTEM

**Hirokage OGOSHI*, Youichi YAMAGUCHI**, Sachio SUZUKI***
***Kawasaki Heavy Industries, Ltd.**
****National Institute of Information and Communications Technology**

**Keywords**: *aerodynamics, wind tunnel test, wake survey*

## Abstract

*This paper shows the Kawasaki wake survey system based on the wake integral method [1][2][3] to obtain the aerodynamic forces acting on a wind tunnel test model. The wake integral method is recognized as an extremely useful flow diagnostic tool for the aerodynamic design of aircrafts, because it can evaluate the spanwise distribution of lift and drag, and separate the profile drag, the induced drag and the wave drag from the total drag [1].*

*We have developed our own Wake Survey Systems for two types of wind tunnels, the Kawasaki Low speed continuous Wind Tunnel (KLWT) and the Kawasaki Transonic Wind Tunnel (KTWT). The wake survey system for KTWT is the unique one in the world which can achieve high data productivity in spite of the short duration time of the blow down type wind tunnel.*

*Several wind tunnel tests were performed in order to evaluate the effectiveness of these new wake survey systems, and the test results show that our wake survey systems can provide extremely useful data for the aerodynamic design in a realistic testing time.*

## 1 Introduction

Although the most usual method to measure the aerodynamic forces acting on a wind tunnel test model is by balance, it is also possible to obtain the aerodynamic forces by measuring the model wake and processing the flow field data. The big merit of a wake survey analysis is that it can evaluate the spanwise distribution of lift and drag, and separate the profile drag, the induced drag and the wave drag from the total drag [1]. These derived drags make it possible to analyze the effect of the model configuration changes on the drag components. So, this method is recognized as an extremely useful flow diagnostic tool for the aerodynamic design of aircrafts, because these analyses are impossible by ordinary measurement with balance.

This is why we started the study of the wake survey technique. Our final goal is to develop this technique to the practical testing tool that will be commonly used in the aerodynamic design and the performance-confirming test for the forthcoming development projects. For these years, we have been developing our own wake survey systems by applying the basic philosophy of the wake integral method. Based on these results, two new systems have been developed for two types of wind tunnels. One is for the Kawasaki Low speed continuous Wind Tunnel (KLWT) and the other is for the Kawasaki Transonic blow down Wind Tunnel (KTWT). The latter system is the unique one in the world which can achieve high data productivity in spite of the short duration blow down type wind tunnel.

## 2 Outlines of KLWT/KTWT

The outlines of KLWT and KTWT, which our wake survey systems are applied to, are explained in this section.

KLWT is the single return closed-circuit wind tunnel. The test section is octagon, and its size is 3.5m x 3.5m for closed cart and 2.5m x 2.5m for open cart. The maximum velocity is 30m/sec for closed cart and 65m/sec for open cart.

KTWT is the blow down type wind tunnel with the test section size of 1m x 1m. The range of Mach number is from 0.2 to 1.4, the range of the stagnation pressure is from 120kPa to 490kPa, and the maximum Reynolds number is about 72 x $10^6$ (at the reference length of 1m and Mach number of 1.0). Wind duration time is from 6sec to 120sec, depending on the test condition.

## 3 Wake Survey System

In developing the wake survey systems for our wind tunnels, we specially considered the system setup easiness and the high measurement efficiency. Each system and the processing of wake survey data are explained in the following.

### 3.1 KLWT Wake Survey System

The wake integral method requires enormous flow field data at the grid points on a wake survey plane. Finding the best spatial interval of data points that satisfies the accuracy and the efficiency of measurement is the key point for the practical use of this method in the Kawasaki wind tunnels.

Therefore, our study started from the examination of the interval of data points in a wind tunnel test. It was appeared that the optimum interval obtained from this test was too small to finish the wake measurement in a realistic time, by using the conventional wake survey system with single probe.

To solve this situation, a rake consisted of 10 spherical five-hole probes was developed. The probes are in a line at regular intervals of 50mm, and a diameter of tip sphere of each probe is 6mm. This rake system is position-controlled by 3-axis traverser set above the test section. By using this rake system, the measuring time is reduced to 1/10 of the previous single probe system. This system can be further improved in the measurement time reduction by replacing the current mechanical-scan pressure measurement system with electro-scan one. The installed wake survey system in KLWT is shown in Fig. 1.

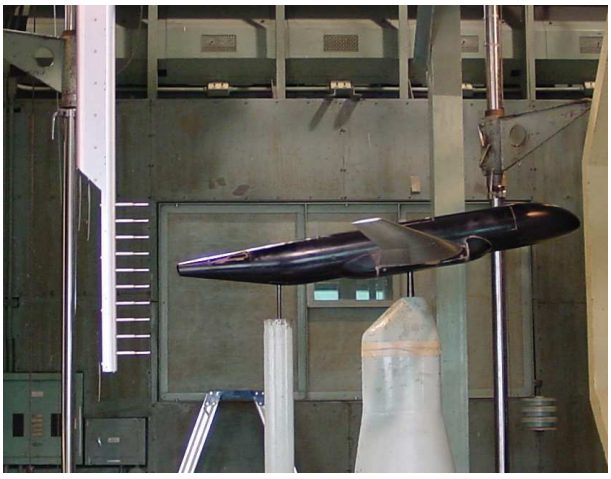

Fig. 1. Wake Survey System in The Kawasaki Low Speed Continuous Wind Tunnel.

### 3.2 KTWT Wake Survey System

#### *3.2.1 Multi-probe for KTWT*

In order to aim at practical use of wake integral method for the aerodynamic design of the aircrafts, the first wake survey test in KTWT had been tried. The measuring system still consisted of a single five-hole probe. And it took about 80 blows (almost 10 days) to measure one wake survey plane, because the wind duration time is very short (maximum 2 minutes). This is the first problem of developing KTWT wake survey system.

To solve this problem, a new system based on previous experience of the KLWT system was developed. The new wake-measuring instrument is a rake consisted of 21 pyramidal five-hole probes of 3.5mm diameter and at regular intervals of 20mm, with the electro-scan type pressure measurement system.

#### *3.2.2 Way of Traversing*

The typical way to obtain the model wake data is to traverse the pneumatic probe in the downstream of the model with the model fixed at a certain position. This is the same way as the KLWT wake survey system. Supposing this method is applied to KTWT, either of the followings is necessary; setting wake measuring probe on the sting strut, or introducing another traversing apparatus. In KTWT, the sting strut is the only mechanism to be used as a traverser, but it is usually used for supporting the model.

The existing wake survey system is designed to be installed to the sting strut. So, if we use this system in the wake survey test, another preparation time is needed to change the model from sting strut support to another support, such as plate-mount support. And if a special traversing apparatus is introduced, an extra controlling system for the apparatus must be needed to the existing measurement and controlling system. As a result, the system becomes more complex. This is the second problem.

We solved this problem by such a new idea about the wake traverse way as the following. The model is supported by the sting strut in the same way as the daily force measurement setup, and the rake is fixed on the wind tunnel floor. The wake data is acquired by the model moving up and/or down in front of the rake to vary the relative position between them. An efficient wake data acquisition is realized by the combination of the multi-probe rake and the new way of traversing. The installed wake survey system in KTWT is shown in Fig. 2.

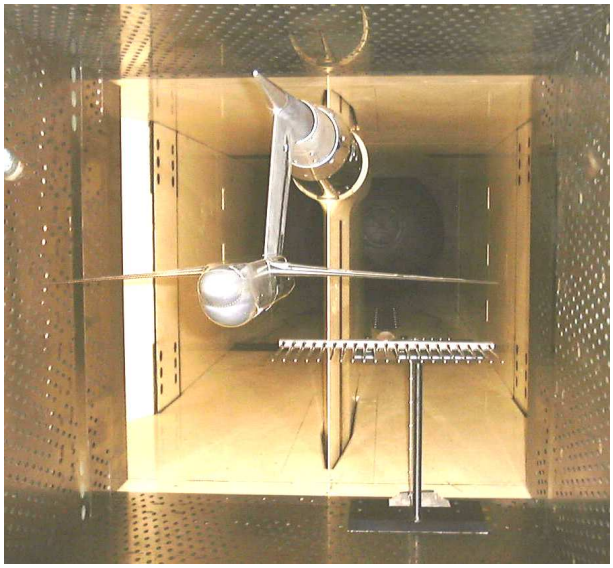

Fig. 2. Wake Survey System in The Kawasaki Transonic Blow Down Wind Tunnel.

### 3.3 Processing of Wake Survey Data

The wake integral method is the well-known method that can calculate the two-dimensional drag acting on the model by integrating total pressure loss along a vertical line behind the model (Betz [4], et al.). Our wake survey systems are based on the expansion of this method which was originated by Maskell [5], and developed for the practical use by Kusunose, et al [1][2][3].

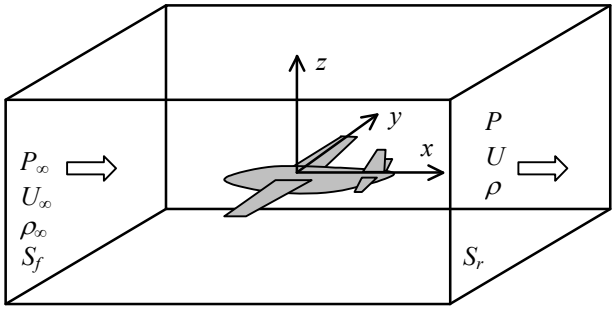


Fig. 3. The Model and The Control Volume.

The forces acting on the model can be estimated from flow field data measured in the downstream wake survey plane *Sr*. The drag *D* can be estimated by the following integral.

$$D = \iint_{Sr} \frac{P_\infty}{R}\left(s - s_\infty\right) dy\, dz + \iint_{Sr} \frac{\rho_\infty}{2}\left(v^2 + w^2\right) dy\, dz \qquad (1)$$

where $P_\infty$ denotes free stream static pressure, $R$ gas constant, $s$ entropy, $v$ and $w$ velocities in $y$ and $z$ direction respectively and $\rho_\infty$ free stream density.

The first integral term yields the drag component called ‘profile drag (*Dp*)’, which includes ‘wave drag (*Dw*)’ caused by occurring shock wave. And the second term yields the drag component called ‘induced drag (*Di*)’. A shock wave will never generate the vorticity in a flow field. So, the vorticity will exist only in the region of total pressure loss caused by the model surface boundary layer. Using this principle, the wave drag component can be extracted from the profile drag [1].

In the practical application of this method to our wind tunnel tests, we firstly store the pressure data measured by probes in the converted form of the pressure coefficient on the existing online wind tunnel measurement system. Using the stored data of several test cases, such the post-processes as the data merge

on a wake survey plane and the calculations of the total pressure ratios and the velocity vectors are performed on the off-line system. User operation of this off-line system is very easy by help of GUI. It usually needs less than 5 minutes to finish the wake integral analyses in the post-process from when all the stored pressure data are prepared.

## 4 Application To Wind Tunnel Testing

Several tests employing the developed wake survey system were performed. Typical wake survey results are described in this section.

### 4.1 Low-speed Test Data at KLWT

#### *4.1.1 Determination of Spatial Interval of Data Points*

At the beginning of this section, we summarize the preliminary test for determination of a spatial interval of the data points. The model was wing-body of typical transport plane, and full span of the wing was 1.6m. Free stream velocity $U_\infty$ was 30m/s, and angle of attack $\alpha$ was 2.5deg. In this case, $C_L$ of the model was approximately 0.42. Wake survey plane was positioned 100mm downstream from the aft end of the fuselage. Wake-measuring were performed with the previous single spherical five-hole probe. And it took approximately 13 hours to acquire one wake survey plane.

Total pressure ratio contours in several intervals of the data points are shown in Fig. 4. A large region of total pressure loss is recognized below the wake from the fuselage. This loss is due to the model-supporting strut. Almost all the part of the strut is covered with the fairing, but there is a part of naked cylindrical strut just below the model (see Fig. 1). This naked strut caused large portion of total pressure loss. Consequently, region of the wake regarded as originated from the strut was excepted from wake analyses region.

In the case of the interval of 10mm, the wing wake is distributed continuously. In the case of the interval of 15mm, the wing wake becomes intermittently. And in the case of 30mm, intermittence becomes extreme, and the wing tip vortex can no longer be recognized.

Comparisons of $C_L$ and $C_D$ between the wake survey data and the balance data are shown in Fig. 5 and Fig. 6, respectively. The induced drag coefficient $C_{Di}$ of the balance case is possible to predict from $C_L$ and aspect ratio of the model. This predicted $C_{Di}$ and that estimated from the wake survey are also plotted in Fig. 6. In the case of the interval of 15mm or less, the

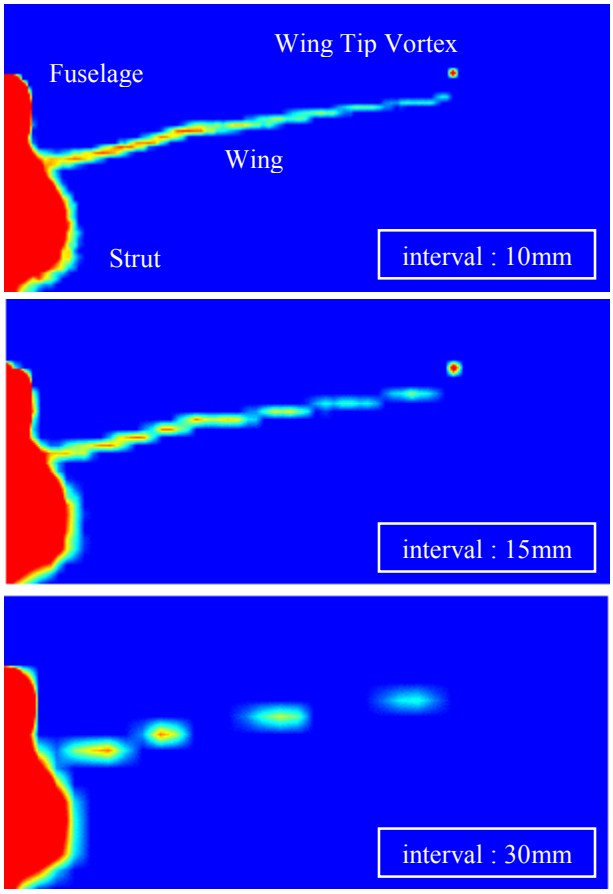


Fig. 4. Total Pressure Contour Comparisons in Several Spatial Intervals of Data Points.

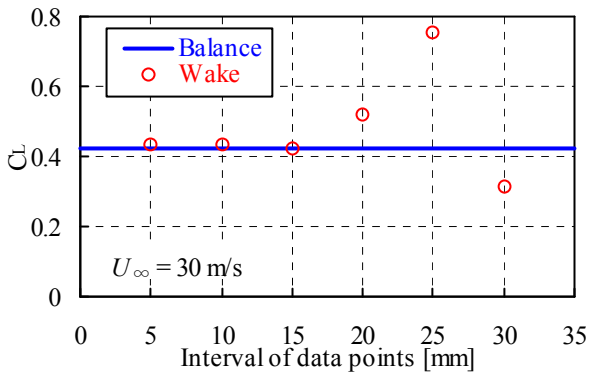


Fig. 5. Effect of The Spatial Interval of Data Points for Lift Analysis.

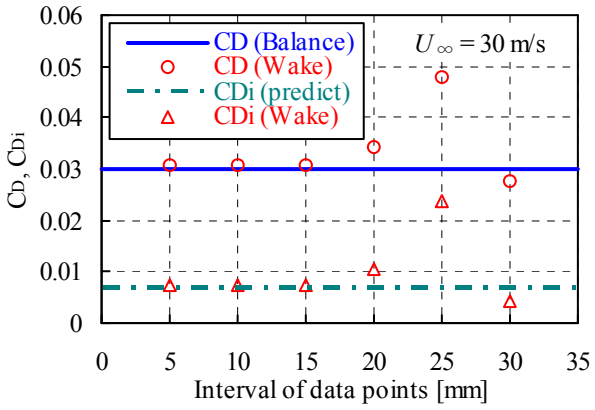


Fig. 6. Effect of The Spatial Interval of Data Points for Drag Analysis.

results of wake survey agree well with the balance data. According to these results, the optimum interval of data points was determined to be 10mm.

### *4.1.2 Contours of Total Pressure Ratio and Vorticity*

After here, the tests performed with the multi-probe wake survey system are described. The model was wing-body of typical transport plane (see Fig. 1), just the same as preliminary test. Free stream velocity $U_\infty$ was fixed at 50m/s, and angles of attack α were set at -2.8deg., 2.3deg., and 7.6deg. In these cases, $C_L$ of the model were approximately 0.0, 0.4, and 0.8, respectively. Wake survey plane was positioned 100mm downstream from the aft end of the fuselage, and the spatial intervals of the data points were 10mm in both $y$ and $z$ directions. In order to evaluate wake survey analyses, the aerodynamic force acting on the model was also measured by pyramidal balance.

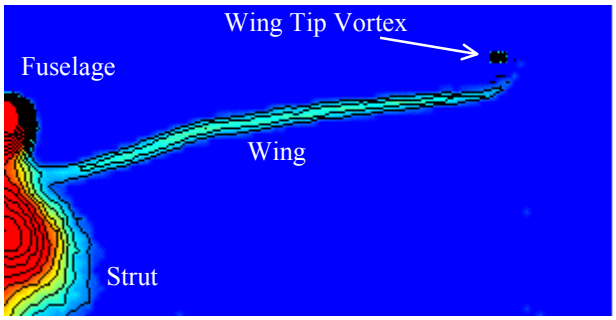


Fig. 7. Total Pressure Ratio Contour. ($U_\infty$=50m/s, α=7.6deg.)

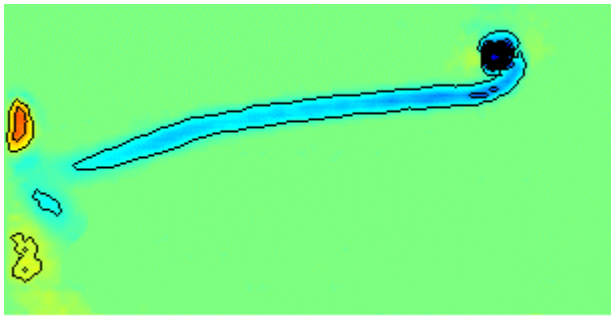

Fig. 8. X Component of Vorticity Vector Contour. ($U_\infty$=50m/s, α=7.6deg.)

The contour maps of the measured total pressure ratio and $x$ component of the vorticity vector on the wake survey plane are showed in Fig. 7 and Fig. 8, respectively. It took approximately 80 minutes to acquire one wake survey plane data. In these figures, the wakes from the fuselage and the wing, and the wing tip vortex are distinguished by this wake survey system.

### *4.1.3 Spanwise Lift and Drag Distributions*

The spanwise lift and drag distributions that are

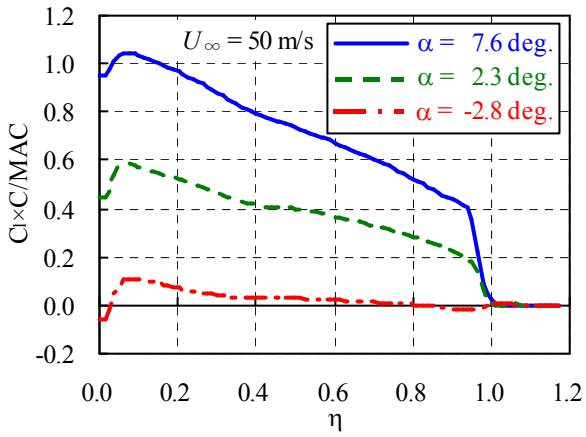


Fig. 9. Spanwise Lift Distributions at Several Angles of Attack.

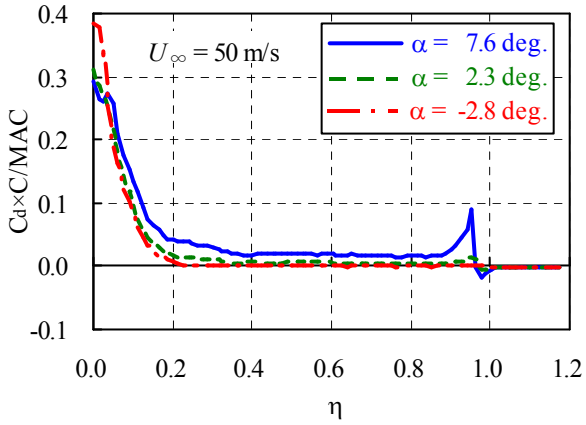


Fig. 10. Spanwise Drag Distributions at Several Angles of Attack.

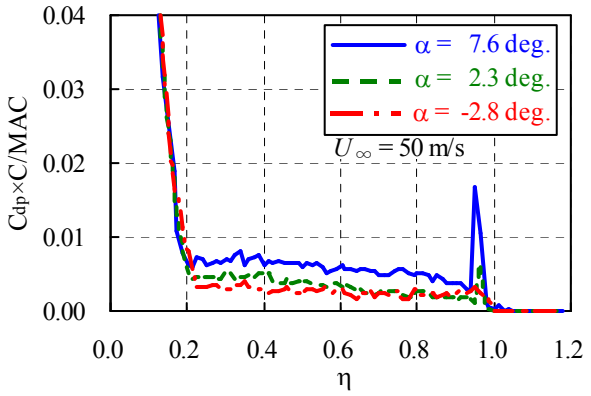


Fig. 11. Spanwise Profile Drag Distributions at Several Angles of Attack.

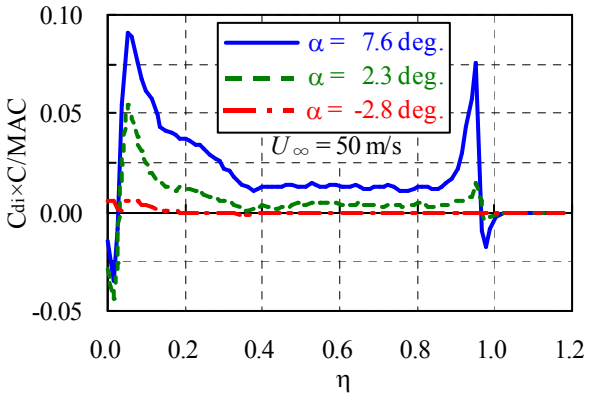


Fig. 12. Spanwise Induced Drag Distributions at Several Angles of Attack.

obtained by this wake survey system are shown in Fig. 9 and Fig. 10, respectively. $C_l$ and $C_d$ denote the wing section lift and drag coefficient, C local wing chord, and MAC mean aerodynamic chord. The profile drag and the induced drag, which are separated from the total drag, are shown in Fig. 11 and Fig. 12. $C_{dp}$ and $C_{di}$ represent the wing section profile drag and the wing section induced drag.

In Fig. 11, taking notice of the distribution at a range of $\eta > 0.5$, no great difference is observed between $C_{dp}$ at $\alpha = -2.8$ deg. and $\alpha = 2.3$deg. At the case of $\alpha = 7.6$deg., $C_{dp}$ level increases as compared with another two cases. This fact indicates that boundary layer thickness increases rapidly, or boundary layer separates from the surface of the wing at $\alpha = 7.6$deg. From Fig. 9 and Fig. 12, $C_{di}$ depended on the gradient of $C_l$ distribution in $\eta$ direction. This fact indicates that $C_{di}$ increased with an increase of the lift.

### *4.1.4 Comparison with Balance Data*

The results of $C_L$ and $C_D$ that were calculated from the former spanwise distributions are shown in Fig. 13 and Fig. 14, respectively. In Fig. 13, on the whole, $C_L$ and $C_D$ of the wake survey data make good agreement with the balance data. $C_{Di}$ predicted from the balance data is also plotted in dashed line in Fig. 14. $C_{Di}$ of the wake survey data agrees well with the prediction from the balance data. This result shows that our method to derive the induced drag is proper. Total $C_D$ of the wake survey data is sum of $C_{Dp}$ and $C_{Di}$. It seems that the profile drag analysis is also appropriate.

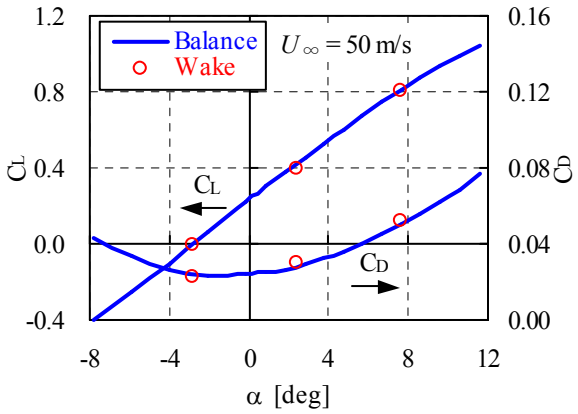


Fig. 13. Comparisons of Lift and Drag between Wake Survey Data and Balance Data in KLWT.

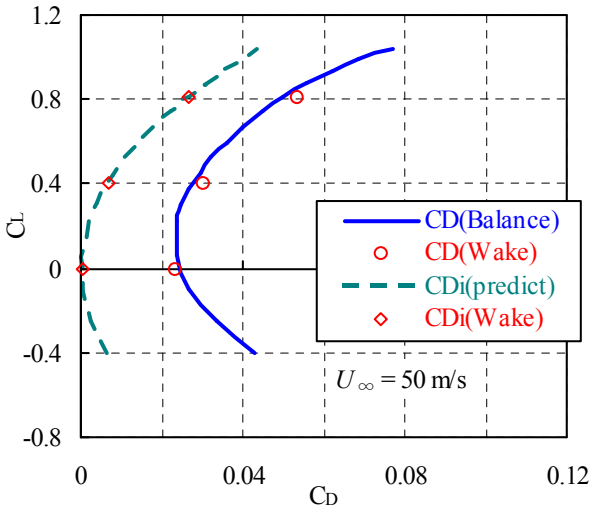


Fig. 14. Comparison of Polar Curve between Wake Survey Data and Balance Data in KLWT.

## 4.2 High-speed Test Data at KTWT

The model was wing-body of typical transonic transport plane (see Fig. 2). At every case, Reynolds number was 1.5 x $10^6$ at the reference chord of MAC. Wake survey plane was positioned 185mm downstream from the aft end of the fuselage, and the spatial intervals of the data points were 5mm in both y and z directions, the value of which was decided based on the KLWT testing results and the model scale. In measuring wake data, the model was moved on pitch and pause mode, and measurements were completed in 4 blows (approximately one hour and a half) for one wake survey plane. Though the measured flow field data includes the support sting wake data, this region was eliminated from wake analyses region in the same manner as KLWT testing. In order to evaluate wake survey analyses, the aerodynamic forces acting on the model were also measured by internal balance.

### *4.2.1 Influence of Model-Move*

As mentioned previous section, KTWT wake survey system measures flow field data by moving the model. Therefore, we studied about the influence of the model position in the test section in several test cases.

These tests were performed at $M$ = 0.8 and $\alpha$ = 1.74deg. $C_L$ and $C_D$ distributions at several model positions are shown in Fig. 15 and Fig. 16, respectively. The results show that $C_L$ depends on the position of the model. However, the perturbation $\Delta C_L$ is less than 0.005 (0.9% of an average value of $C_L$), the change of $C_L$ caused by the model position was not so large.

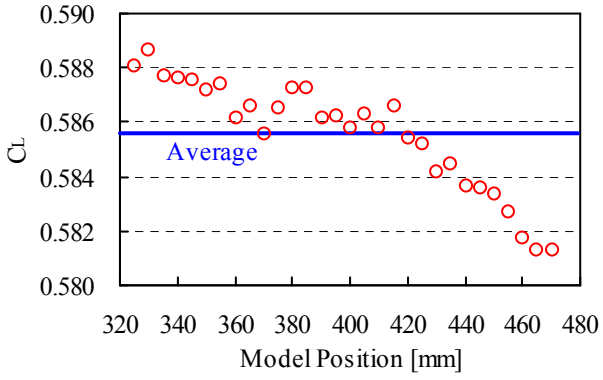


Fig. 15. $C_L$ Distribution at Several Model Position.

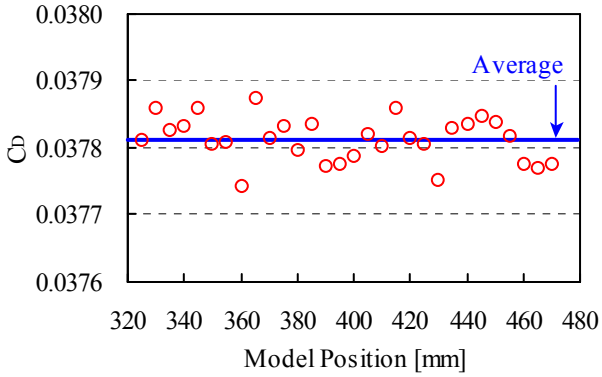


Fig.16. $C_D$ Distribution at Several Model Position.

$C_D$ is not affected by the vertical move of the model so much.

Comparisons between the wake survey data and the balance data are shown in Fig. 17. The balance data were measured by positioning the model at the center of the test section. It is recognized that both of them agree very well.

Therefore, according to these results, the influence of the position of the model on the aerodynamic properties is small, and we can judge that this wake survey analysis functions enough as a diagnostic tool.

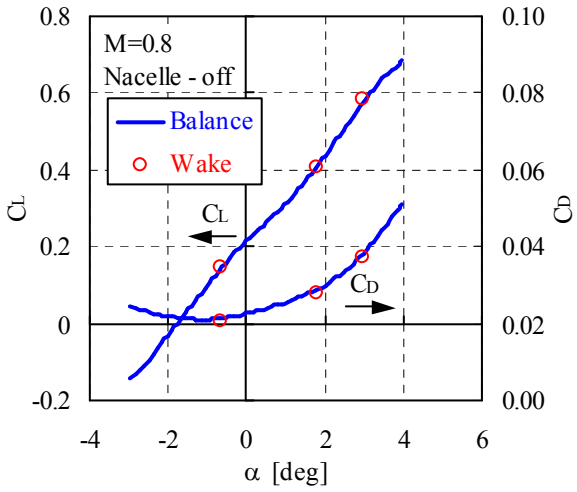


Fig 17. Comparison of Lift and Drag between Wake Survey Data and Balance Data in KTWT.

### *4.2.2 Extraction of Wave Drag from Profile Drag*

Next, we tried to extract the wave drag from the profile drag. In order to evaluate the validity of the wave drag extraction, some criteria are necessary. So we prepared $C_D$-Mach curve at $C_L$ = 0.4 from the balance data, and calculated

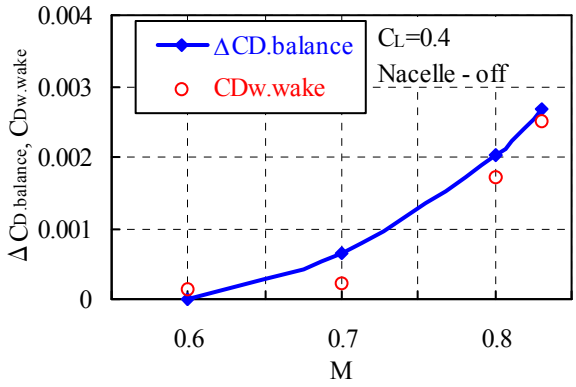


Fig. 18. Comparison between $\Delta C_{D.balance}$ and $C_{Dw}$.

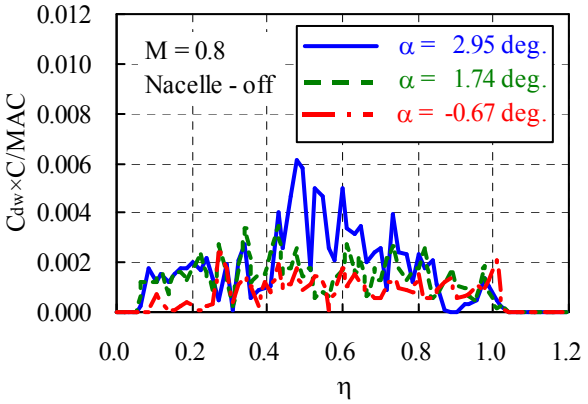


Fig. 19. Spanwise Cdw Distributions.

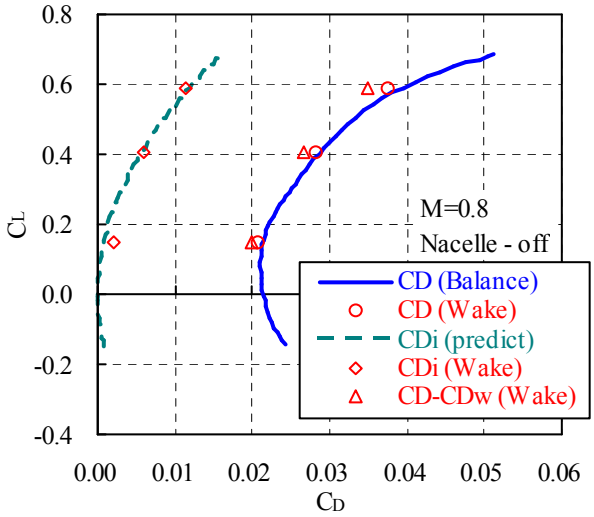


Fig. 20. Comparison of Polar Curve between Wake Survey Data and Balance Data in KTWT.

$\Delta C_{D.balance}$ which is the increment of $C_D$ at each Mach number from $C_D$ at $M$ = 0.6. We utilized this $\Delta C_{D.balance}$ for criterion. Of course $\Delta C_{D.balance}$ does not agree with the wave drag exactly, because it includes not only the wave drag but also the drag caused by the boundary layer separation and perturbation of the induced drag.

$C_{Dw.wake}$, which are extracted from $C_{Dp}$ of the wake data, are plotted with $\Delta C_{D.balance}$-Mach curve in Fig. 18. It is recognized that $C_{Dw.wake}$ does not increase where the Mach number is under 0.7, and increase where the Mach number is beyond 0.7. From these results, the tendency of the wave drag can be estimated appropriately by the wake survey analyses.

Next wake survey results for angles of attack of -0.67deg., 1.74deg., and 2.95deg. at fixed free stream Mach number of 0.8 are shown in Fig. 19 and Fig. 20. In these cases, $C_L$ of the model are approximately 0.15, 0.41 and 0.59, respectively. As seen in Fig. 19, wing section wave drag is increase at $\eta > 0.4$ in the case of $\alpha = 2.95$deg. As seen in Fig. 20, wake survey analyses capture the tendency that wave drag is increase with increase of $C_L$.

### *4.2.3 Effect of Configuration Changes on Air Load Components*

We confirmed the ability of the wake survey analyses to estimate the effect of the appendage. For that purpose, flow-through nacelles are appended to the model (see Fig. 21). The total pressure ratio contour map and $x$ component of the vorticity vector contour map are shown in Fig. 22 and Fig. 23, respectively.

The nacelle effects on the spanwise lift distribution at a constant free stream Mach number ($M$ = 0.8) condition are shown in Fig.

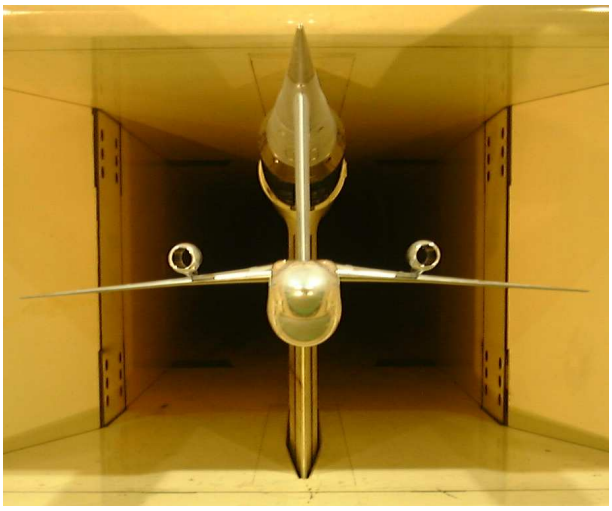

Fig. 21. The Model with Nacelles for KTWT Wake Survey.

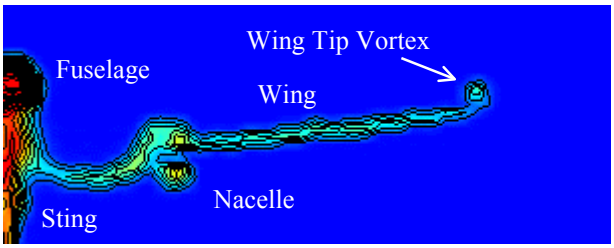


Fig. 22. Total Pressure Ratio Contour.
($M$=0.8, $C_L$=0.40, Nacelle-on)

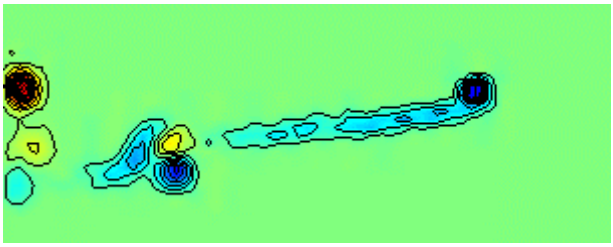

Fig. 23. X Component of Vorticity Vector Contour.
($M$=0.8, $C_L$=0.40, Nacelle-on)

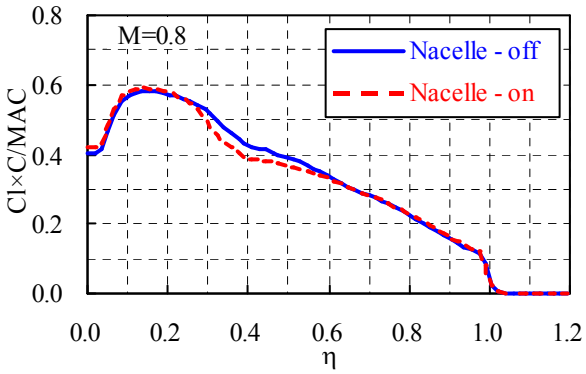


Fig. 24. Comparison of Spanwise Lift Distributions between Nacelle-off and Nacelle-on Conditions.

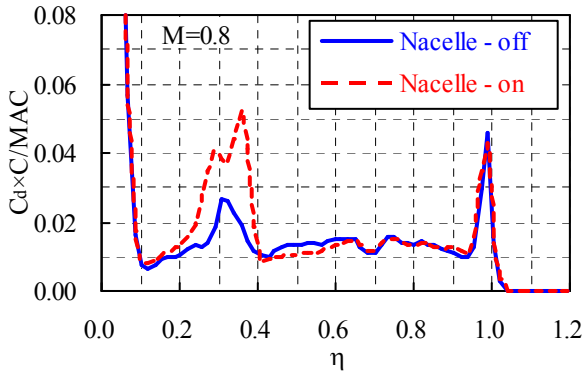


Fig. 25. Comparison of Spanwise Drag Distributions between Nacelle-off and Nacelle-on Conditions.

24. $C_L$ of the model was 0.41 at nacelle-off condition and 0.40 at nacelle-on condition. Lift loss due to the nacelle is seen around η = 0.4. Fig. 25 shows the corresponding spanwise drag

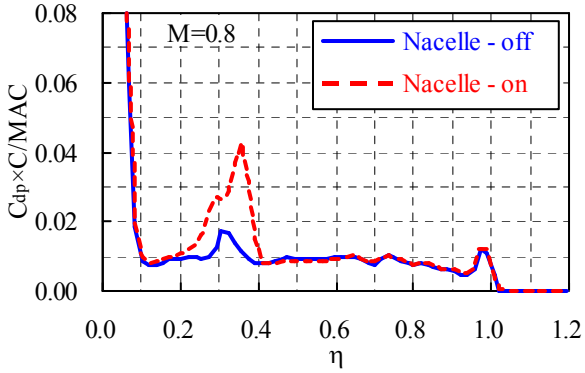


Fig. 26. Comparison of Spanwise Profile Drag Distributions between Nacelle-off and Nacelle-on Conditions.

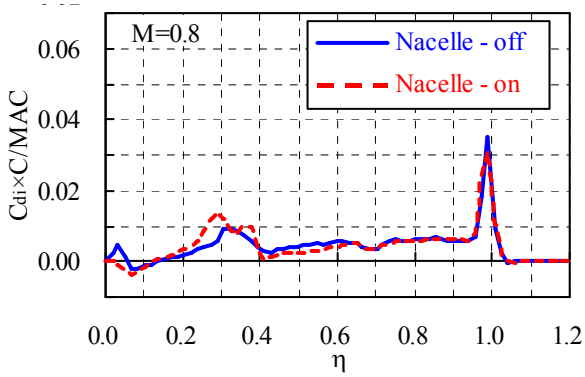


Fig. 27. Comparison of Spanwise Induced Drag Distributions between Nacelle-off and Nacelle-on Conditions.

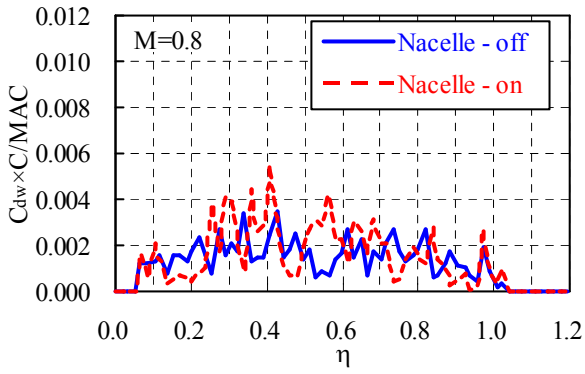


Fig. 28. Comparison of Spanwise Wave Drag Distributions between Nacelle-off and Nacelle-on Conditions.

distributions. Significant increase of the drag due to the nacelle is observed. The spanwise profile drag, induced drag, and wave drag are shown in from Fig. 26 through Fig. 28. From these figures, the effect of the nacelle mainly appears in the profile drag. The increases of the induced drag and the wave drag are slight.

Table 1. Comparisons between Wake Survey Data and Balance Data on Nacelle Effect.

| | $\Delta C_D$ | $\Delta C_{Dp}$ | $\Delta C_{Dw}$ | $\Delta C_{Di}$ |
|---|---|---|---|---|
| Balance | 0.00234 | - | - | - |
| Wake | 0.00240 | 0.00237 | 0.00024 | 0.00003 |

The drag comparisons between the wake survey data and the balance data are shown in Table 1. $\Delta C_D$ means the difference of $C_D$ between the nacelle-on and the nacelle-off conditions. $\Delta C_D$ calculated from the wake survey data agrees quite well with the balance data. The details of $\Delta C_D$ from wake survey are also shown in Table 1 for reference.

From these results, wake survey is possible to estimate quantitative effects of the appendage against the aerodynamic property and specify a region and a degree of its influence. The method of the wave drag extraction, especially quantitative valuation of the wave drag, will be kept on studying with making use of the CFD results.

## 5 Conclusions

We have developed the wake survey systems for KLWT and KTWT without large-scale change of existing wind tunnel measuring and controlling system.

With the optimum spatial interval of measuring grid and the multi-probe rake system, the measurement efficiency was greatly improved from 13 hours to 80minutes in KLWT and from 80 blows to 4 blows in KTWT.

For both of KLWT wake survey system and KTWT wake survey system, agreement of the aerodynamic property from wake data with that of balance data is quite well. The results show that our wake survey systems provide extremely useful data in a realistic testing time. Therefore these systems are very effective equipments for diagnosis of the aerodynamic design of aircrafts.

## Acknowledgement

Our special thanks are due to Dr. Akira FUJIMOTO, Mr. Sei-ichi SONODA and Mr. Hiroaki NIWA for technical suggestions and comments in developing these systems.

## References

[1] Kusunose K, Crowder J P and Watzlavick R L. Wave drag extraction from profile drag based on a wake-integral method. *37th AIAA Aerospace Sciences Meeting & Exhibit*, Reno, Nevada, AIAA-99-0275, 1999.

[2] Kusunose K. Drag prediction based on a wake-integral method. *16th AIAA Applied Aerodynamics Conference*, Albuquerque, New Mexico, AIAA-98-2723, 1998.

[3] Kusunose K. Lift analysis based on a wake-integral method. *39th AIAA Aerospace Sciences Meeting & Exhibit*, Reno, Nevada, AIAA-2001-0420, 2001.

[4] Betz A. Ein verfahren zur direkten ermittlung des profilwiderstandes. *Zeitschrift für Flugtechnik und Motorluftschiffahrt*, Vol.16, pp.42-44, 1925.

[5] Maskell E C. Progress towards a method for the measurement of the components of the drag of a wing of finite span, *Royal Aircraft Establishment Technical Report 72232*, 1972.